

# Controller Design for a Nozzle-flapper Type Servo Valve with Electric Position Sensor

Iwan Istanto<sup>1</sup>, Ill-yeong Lee<sup>2\*</sup>, Jun-young Huh<sup>3</sup> and Hyun-cheol Lee<sup>4</sup>

Received: 8 Feb. 2019, Accepted: 19 Feb. 2019

**Key Words** : Servo Valve, Electric Position Feedback, Control Performance, Oscillation Phenomenon

**Abstract:** The control performance of hydraulic systems is basically influenced by the performance of electrohydraulic servo valve incorporated in a hydraulic control system. In this study, a control design was proposed to improve the control performance of a servo valve with a non-contact eddy current type position sensor. A mathematical model for the valve was obtained through an experimental identification process. A PI-D control together with a feedforward (FF) control was applied to the valve. To further improve the dynamic response of the servo valve, an input shaping filter (ISF) was incorporated into the valve control system. Finally, the effectiveness of the proposed control system was verified experimentally.

## Nomenclature

$d_e$  : disturbance  
 $K_P$  : proportional gain  
 $K_I$  : integral gain  
 $K_D$  : differential gain  
 $p_l$  : load pressure  
 $p_s$  : supply port pressure  
 $p_t$  : tank port pressure  
 $u, u_d$  : control inputs shown in Fig. 5  
 $x_s$  : spool position  
 $x_r, x_{ref}$  : reference inputs shown in Fig. 5  
 $\zeta$  : damping ratio in Eq. (1)  
 $\omega_n$  : natural frequency in Eq. (1)

## 1. Introduction

Electro-hydraulic servo valves have been used for controlling hydraulic systems for a long time. The object servo valve under study is a nozzle-flapper type two-stage servo valve. The valve has a feedback spring mechanism for spool position feedback. The servo valve used in this study has an additional electric position sensor with non-contact eddy current type as shown in Fig. 2. Electro-hydraulic servo valves with electric position sensor are currently available commercially<sup>1-2)</sup>.

In the case of servo valve with an electric position sensor, control system designers can actively intervene in the control action of the servo valve control loop, unlike in the case of the valve without an electric position sensor<sup>3-4)</sup>. However, the information on the control scheme of the valves with additional electric position sensor is not open to general hydraulic control engineers, and also the performance limitations of the valves are not known. These points are the motivation for this study.

Prior to the controller design for the servo valve, the mathematical model of the servo valve is obtained through a preliminary experiment of the frequency response characteristics of the valve without electric

\* Corresponding author: iylee@pknu.ac.kr

1 Graduate school, Pukyong National University, 48513 Korea (BPPT Indonesia)

2 Pukyong National University, Korea

3 Korea University of Technology and Education, Korea

4 SG Servo Co., Korea

Copyright © 2019, KSFC

This is an Open-Access article distributed under the terms of the Creative Commons Attribution Non-Commercial License(<http://creativecommons.org/licenses/by-nc/3.0>) which permits unrestricted non-commercial use, distribution, and reproduction in any medium, provided the original work is properly cited.

feedback control.

To achieve a robust reference following control while rejecting the effects of the disturbances, a reference following controller (including PI-D and feed-forward controller) is designed using the pole placement method and the zero placement method<sup>5-7</sup>. Also, it is known that the input shaping filter(ISF) which is positioned outside the feedback control loop in control systems can modify the entire loop transfer function, without deteriorating the function of the control loop for disturbance rejection<sup>6-9</sup>. So far, however, studies applying ISF for improving the control performance of hydraulic servo valves are hardly found. In this paper, therefore, the authors propose a control design using ISF for improving the control performance of the servo valve in the high-frequency range. The effectiveness of the proposed control design is verified experimentally.

## 2. Mathematical modeling of the servo valve

### 2.1 Overview of the servo valve controlled system

Fig. 1 shows the configuration of the control system for the servo valve under study. The system consists of a servo valve, a servo amplifier and a controller (personal computers). The servo valve is a nozzle-flapper type valve with a two-stage structure, which was manufactured by SG Servo Co. in Korea. The servo amplifier has a minor control loop for current feedback control. Gain adjusting, null adjusting and dither input setting can be done on the servo

amplifier. The controller (personal computers) carries out system control and experimental data acquisition.

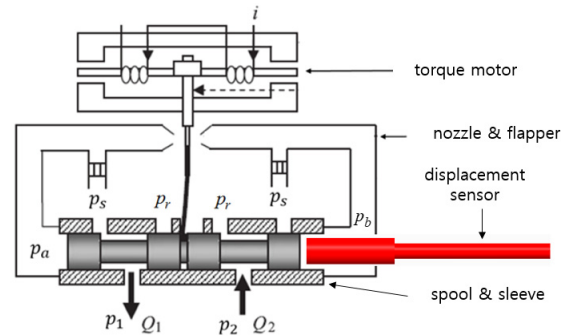


Fig. 2 Structure of the servo valve

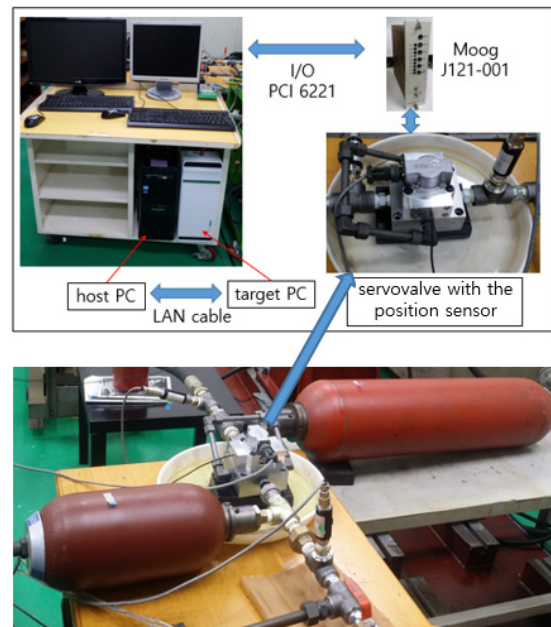


Fig. 3 Photograph of the experimental system of the servo valve

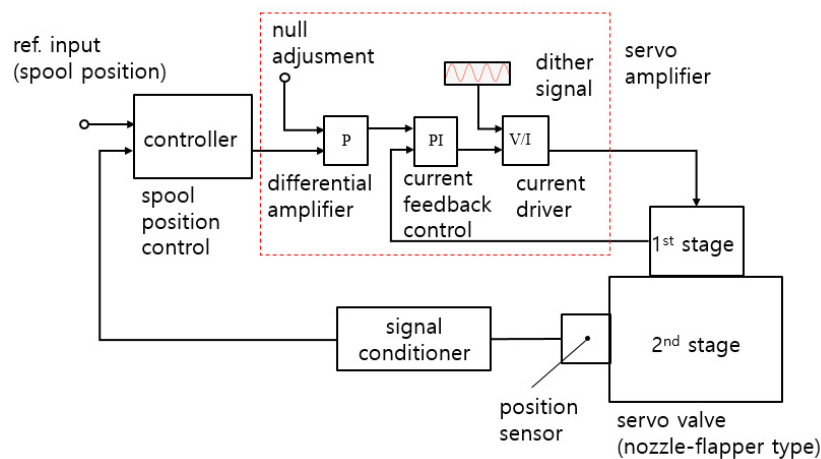


Fig. 1 Block diagram of the control system for the servo valve

Fig. 2 shows the structure of the servo valve under study, where an eddy current type position sensor (Keyence AH-305) is installed.

Fig. 3 shows photographs of the key parts of the experimental system. The experiments on the control performance of the valve are performed under no load condition throughout this study, therefore the actuator ports (A and B ports) of the valve are directly connected using a steel pipe. To maintain the pressure at the P port and the T port of the valve at a constant value during the dynamic characteristics test of the valve, bladder type accumulators (upstream side: 30 L, downstream side 10 L) were used, The gas charge pressures (gauge pressure) were 60 bar and 0.2 bar, respectively.

Simulink Real-Time(SLRT)<sup>11)</sup> is applied to perform control actions and collect experimental data on the controller(two personal computers). For the implementation of SLRT, the host PC and the target PC is connected by a LAN cable. The control frequency of the SLRT is 20 kHz (discretizing time of 0.05 ms).

Table 1 shows specifications of major components of the system shown in Fig. 1.

Table 1 Specifications of the major components of the system shown in Fig. 1

<p><b>Servo valve(SG Servo co.)</b>                  rated flowrate: 63L/min @<math>P_s=210</math>bar,                  rated current (when coil connected in parallel): 40mA</p>
<p><b>Servo amplifier(Moog J121-001)</b>                  input range: <math>\pm 10</math>VDC, dither frequency: 320Hz</p>
<p><b>Position Sensor(Keyence AH-305)</b>                  measurement range: 0~1mm, resolution: 1<math>\mu</math>m,                  response(@-3dB): 3.3kHz</p>
<p><b>Controller(PC)</b>                  ASUS P8H61-M with intel core i5-2500K</p>
<p><b>Interface card(NI 6221)</b>                  resolution(AI, AO): 16bit, input-output range:  <math>\pm 10</math>VDC, signal bandwidth(@-3dB): 700kHz</p>

### 2.2 Modeling of the servo valve

The static and dynamic characteristics of the nozzle-flapper type servo valves are described by the basic equations consisting of a torque balance equation

in the armature of the torque motor, a continuity equation in the chambers inside the nozzles, an equation of motion of the spool<sup>12)</sup>. These basic equations are complex nonlinear differential equations, which include physical parameters those are not easy to measure, such as bulk modulus of oil, flow force coefficient in the spool throttle flow, flow force coefficient in the nozzle jet flow, and the frictional coefficient in the spool dynamics. Therefore, it is very difficult to obtain a practical mathematical model for use in control system design. In this study, a transfer function with the standard second order form is obtained through a preliminary experiment using the servo valve, considering its' applicability to control system design.

Fig. 4 is a Bode diagram obtained from a preliminary experiment. The experimental conditions are summarized as follows; an open-loop control (without electric position sensor signal), the supply current  $i = 0.4 i_r \sin \omega t$  ( $i_r = 40$ mA), the supply pressure  $p_s : 70$  bar, the load pressure  $p_l : 0$  bar. From the bode diagram, an open-loop transfer function  $G_{v-open}(s)$  is approximated with Eq. (1).

$$G_{v-open}(s) = \frac{\omega_n^2}{s^2 + 2\zeta\omega_n s + \omega_n^2} \tag{1}$$

$$= \frac{250000}{s^2 + 900s + 250000}$$

$$[\zeta \cong 0.9, \omega_n \cong 500]$$

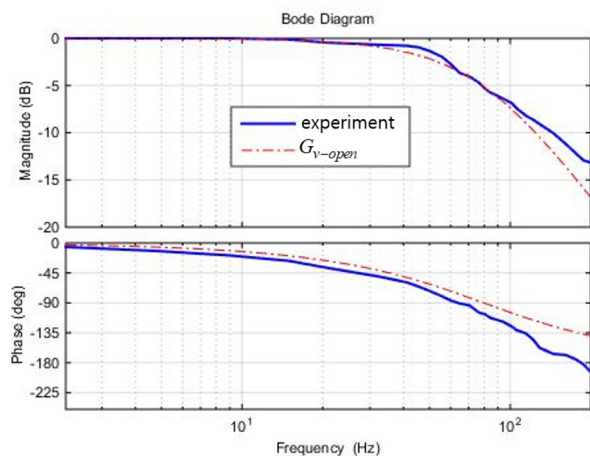


Fig. 4 Bode diagram of the servo valve without electric position sensor ( $i = 0.4 i_r \sin \omega t, i_r = 40$  mA)

### 3. Controller design

In this study, the authors establish the following specifications on the control performances for the servo valve<sup>13</sup>.

1) Under the step disturbance due to steady state flow force, the error in spool position  $x_s(t)$  converges to 0.03 mm in 0.01 s.

2) Under a step input, the maximum overshoot is within 5 % of the final value of  $x_s(t)$ , and the rise time  $t_r$  (the time for  $x_s(t)$  response from 0 to 90 % of  $x_s(\infty)$ ) is within 0.005s.

3) Under a step input, the steady state error is 0. In this study, the control system shown in Fig. 5 shall be designed so that the servo valve can meet the specifications on the control performance described above. In Fig. 5,  $G_{v-open}(s)$ ,  $G_{PI}(s)$ ,  $G_D(s)$ ,  $G_{FF}(s)$ ,  $G_{ISF}(s)$  and  $G_{filter}(s)$  show the transfer functions of a servo valve, a proportional-integral(PI) controller, a differential(D) controller, a feed-forward (FF) controller, an input shaping filter (ISF) and a low-pass filter, respectively.  $G_{filter}(s)$  is incorporated to exclude unwanted high-frequency signal (mainly due to the dither signal) in  $x_s(t)$ .  $d_e(t)$  is disturbance including the dither signal.  $k_d$  is a constant for describing the relationship between  $d_e(t)$  and  $u_d(t)$ , and it is identified with  $k_d \cong 0.114V/N$ .  $u_d(t)$  is the control input due to  $d_e(t)$ . The procedure to design the control system is described below.

#### 3.1 PI-D control

In Fig. 5, the transfer function between the disturbance input  $u_d(s)$  and the spool position  $X_s(s)$  is

$$\frac{X_s(s)}{u_d(s)} = \frac{G_{v-open}(s)}{1 + G_{v-open}(s)(G_{PI}(s) + G_D(s))}. \quad (2)$$

By defining  $G_{PI}(s) = K_P + K_I/s$ ,  $G_D(s) = K_D s$ , and using Eq. (1) for  $G_{v-open}(s)$ ,  $X_s(s)/u_d(s)$  is described as

$$\begin{aligned} \frac{X_s(s)}{u_d(s)} &= \frac{G_{v-open}(s)}{1 + G_{v-open}(s)(G_{PI}(s) + G_D(s))} \\ &= \frac{\beta \omega_n^2 s}{s^3 + (2\zeta \omega_n + \beta \omega_n^2 k_D) s^2 + (\omega_n^2 + \beta \omega_n^2 k_p) s + \beta \omega_n^2 k_I} \\ &= \frac{250000s}{s^3 + (900 + 250000k_D) s^2 + (250000 + 250000k_p) s + 250000k_I}. \end{aligned} \quad (3)$$

By placing the poles of Eq. (3) to  $[-1700+10j, -1700-10j, -255]$  so as to satisfy the design specifications on disturbance rejection, the PI-D gains are determined as

$$K_p = 13.62, \quad K_I = 2601 \quad \text{and} \quad K_D = 0.0109. \quad (4)$$

#### 3.2 FF-PI-D control

From Fig. 5, the transfer function  $X_s(s)/X_r(s)$  is described as

$$\frac{X_s(s)}{X_r(s)} = \frac{(G_{PI}(s) + G_{FF})G_{v-open}(s)}{1 + (G_{PI}(s) + G_D(s))G_{v-open}(s)}. \quad (5)$$

Let's describe  $G_{FF}(s)$  as

$$G_{FF}(s) = c_1 s + c_2. \quad (6)$$

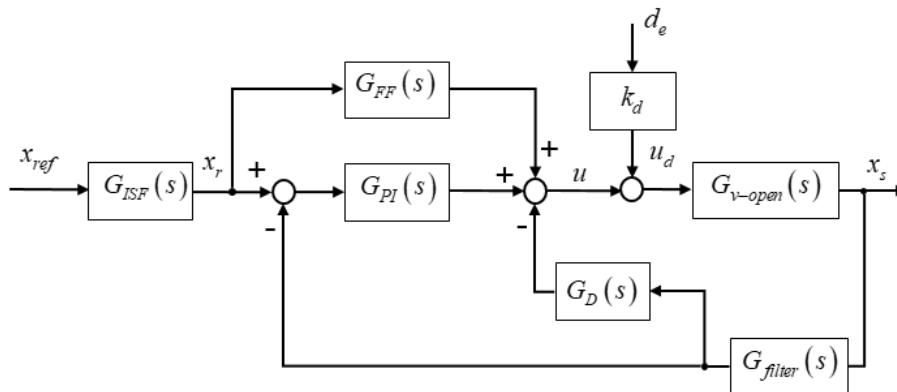


Fig. 5 Block diagram of the control system

From Eq. (1), (4) and (6), we obtain the following equation.

$$\frac{X_s(s)}{X_r(s)} = \frac{\left[ \left( 13.62 + \frac{2601}{s} \right) + (c_1s + c_2) \right] 250000s}{s^3 + 3625s^2 + 3.65 \times 10^6 s + 6.5 \times 10^8} \quad (7)$$

By applying the zero placement method<sup>5-7)</sup>, that is, by equating the numerator and the last three terms of the denominator of Eq. (5),  $G_{FF}(s)$  can be determined to be

$$G_{FF}(s) = 0.014s + 1. \quad (8)$$

Therefore, Eq. (5) is described as

$$\frac{X_s(s)}{X_r(s)} = \frac{3625s^2 + 3.65 \times 10^6 s + 6.5 \times 10^8}{s^3 + 3625s^2 + 3.65 \times 10^6 s + 6.5 \times 10^8} \quad (9)$$

### 3.3 ISF-FF-PI-D control

The control performances of servo valves are generally shown by bandwidth in a Bode diagram. To reform the Bode diagram of the FF-PI-D controlled system into the desired form, in this study, an input shaping filter (ISF) is appended to the FF-PI-D controlled system designed already. The transfer function of the ISF adopted here has the form of a lead-lag compensator, and is described as

$$G_{ISF}(s) = \frac{(T_1s + 1)}{(T_2s + 1)}. \quad (10)$$

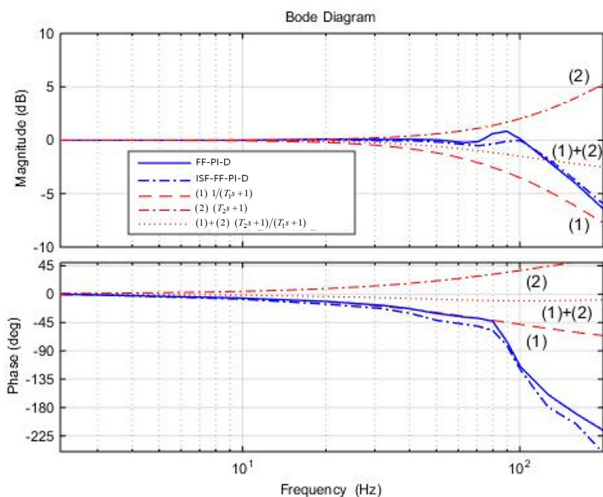


Fig. 6 Design process for the ISF

$G_{ISF}(s)$  was designed with  $T_1=6.36 \times 10^{-3}$  and  $T_2=2.27 \times 10^{-3}$ .  $T_1$  and  $T_2$  can be selected by control designer's intuition together with referring to Fig. 6 so that the ISF can drive the desired modification of the FF-PI-D controlled system<sup>6-7)</sup>.

### 3.4 Low-pass filter

In the hydraulic control system, the dither signal has been used to improve the control performance of the servo valve<sup>14)</sup>. The dither signal can reduce frictional resistance in servo valves. In the servo valve under study, 320 Hz rectangle wave signal with 1 mA amplitude is used as a dither for the open-loop application. In the closed-loop control, the dither signal may induce an undue oscillation to the servo valve. To mitigate the excessive oscillation, a digital low-pass filter with the form of

$$G_{filter}(s) = \frac{1}{Ts + 1} \quad (11)$$

is applied, where the value of  $T=1/1257$ , so as the break frequency of the filter at -3 dB to be 200Hz.

## 4. Control performance of the servo valve

The experimental system is composed as in Fig. 1 and Fig. 3, in which the controller shown in 5 is applied. The controller is implemented on a PC using Matlab Simulink Real-Time (SLRT)<sup>11)</sup> with a discretizing time of 0.05 ms.

In the experiment, the reference input is 40% of the rated input of the servo valve, the supply port pressure ( $p_s$ ) is 70 bar and the tank port pressure ( $p_t$ ) is 0 bar. To the system, a dither signal with 320 Hz and 1 mA amplitude is applied. The amplitude of the dither signal  $\pm 1$ mA corresponds to  $\pm 2.5\%$  of the rated current 40 mA in this valve. In general, the amplitude of the dither signal is determined to be not more than 5% of the rated current of a servo valve<sup>14)</sup>, so a value of 2.5% is not excessive but not underestimated.

### 4.1 Oscillation phenomenon in step response

Fig. 7 shows the experimental result of the step response of the open-loop system without the electric

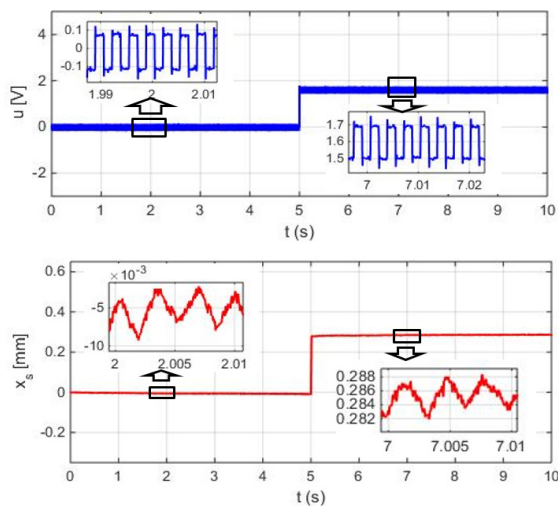


Fig. 7 Step response of the servo valve without electric position feedback signal (open-loop control)

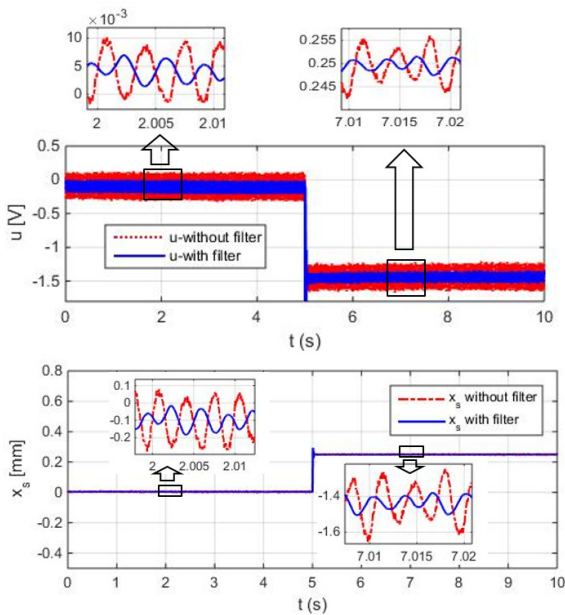


Fig. 8 Step response of the servo valve with electric position signal under the closed-loop control (with/without the digital filter)

position feedback signal using the experimental system shown in Fig. 1 and 3. The experimental result shows that the valve operates normally, and it shows oscillation in the spool displacement with the magnitude of about  $2\mu\text{m}$  due to the dither signal.

Fig. 8 shows the experimental result of the step responses of the system with/without the digital low-pass filter under P control ( $K_p = 6.25$ ). In the case

without the filter, oscillation with big magnitude like 210 mV in  $u$  and  $150\ \mu\text{m}$  in  $x_s$  were observed. After applying the low-pass filter, the oscillation could be moderated to the level of  $50\ \mu\text{m}$  in  $x_s$ .

Applying the dither signal to servo valve is a necessary and very important strategy to reduce static friction between spool and sleeve in a valve. However, when the oscillation in  $x_s$  due to dither signal is fed back to the controller in closed-loop control, the oscillation may result in a one with relatively large amplitude. This fact is clearly demonstrated in Fig. 8. This oscillation phenomenon could be easily solved by the digital filter applied in this study.

#### 4.2 Frequency response

Fig. 9 shows the experimental results of the frequency response of the servo valve under the PI-D, the FF-PID and the ISF-FF-PI-D control using the experimental system shown in Fig. 1 and Fig. 3. To exclude the high-frequency component (the dither signal component) in  $x_s$ , a low-pass filter with the break frequency of 200 Hz was applied to the system.

When the open-loop control and the PI-D control in Fig. 9 are compared, it is noted that the PI-D control contributed to a substantial improvement in the bandwidth [from 60 Hz to 140 Hz], but caused excessive rise of the gain and the phase delay in the high-frequency range. Then, appending FF control to the PI-D control corrected the surplus gain over 0 dB

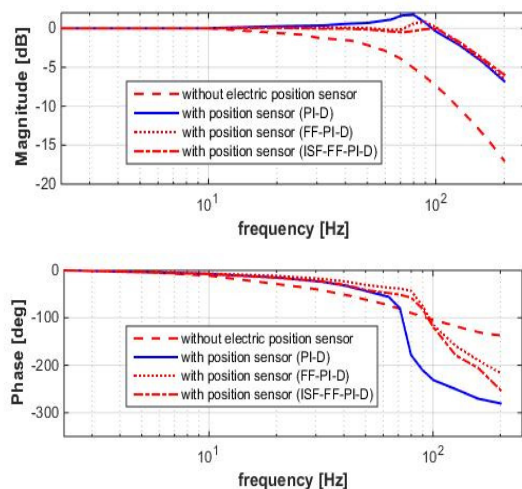


Fig. 9 The frequency response under the PI-D, FF-PID and ISF-FF-PI-D control in the servo valve

Table 2 Summary of the control performances of the servo valve.

items	open-loop	PI-D	FF-PI-D	ISF-FF-PI-D
bandwidth (at -3 dB) [Hz]	60	140	142	146
phase angle(at -3 dB) [deg]	-70.5	-260	-174.5	-195.7
frequency (at -90° phase angle) [Hz]	80	72	94	92
resonance peak	-	1.22 [1.74 dB]	1.10 [0.843 dB]	0.99 [-0.02 dB]

in the high-frequency range and the phase delay in the high-frequency range. Further adding the ISF to the FF-PI-D control contributed to the gain adjustment towards 0dB in the high-frequency range without large damage of the phase angle.

The control performances in the various control schemes are summarized in Table 2.

## 5. Conclusions

In this study, the authors proposed a control design to improve the control performance of servo valves with a non-contact eddy current type position sensor. A mathematical model for the valve was obtained through an experimental identification process. A PI-D controller together with a feedforward (FF) control was applied to the valve. To further improve the dynamic response of the servo valve, an input shaping filter (ISF) was incorporated into the valve control system. It was ascertained from experiments that application of the FF (feed-forward) & the ISF (input shaping filter) control to the PI-D controlled system for the servo valve could remarkably improve the control performance in the frequency response. In addition, it was verified that the oscillation phenomenon induced by feeding back the dither signal involved in the spool position signal could be easily solved by a digital low-pass filter applied in this study.

## Acknowledgement

This work was supported by a Research Grant of Pukyong National University (2017 year).

## References

- 1) Moog Inc., Servo Valves & Pilot Operated Flow Control Valve, January, 2014.
- 2) S. D. Kim, S. H. Son and Y. B. Ham, "Effect of Spool-Sleeve Geometry on Static Pressure Characteristics of Servo Valves", Journal of Drive and Control, Vol.13 No.1, pp.34-42, 2016.
- 3) C. N. Kang et al., "Dynamic Characteristics of Electrohydraulic Proportional Valve for an Independent Metering Valve of Excavator", Journal of Drive and Control, Vol.15, No.2, pp.46-51, 2018.
- 4) S. Kim, S. Jeon and J. Yun, "A Study on the Phase Bandwidth Frequency of a Directional Control Valve based on the Metering Orifice", Journal of Drive and Control, Vol.15, No.1, pp.1-9, 2018.
- 5) K. Ogata, Modern Control Engineering, Prentice Hall, New Jersey, 1997.
- 6) I.-Y. Lee et al., "Control of an Overlap-type Proportional Directional Control Valve Using Input Shaping Filter", Mechatronics, Vol.29, pp.87-95, 2015.
- 7) H.-H. Kim, I.-Y. Lee and J.-Y. Huh, "High-Bandwidth Tracking Control of Electric Hydrostatic Actuator(EHA) Using an Input Shaping Filter", Lecture Notes in Electrical Engineering, Vol.415, pp.97-107, 2016.
- 8) M. Kenison and W. Singhose, "Concurrent Design of Input Shaping and Proportional Plus Derivative Feedback Control", Journal of Dynamic Systems, Measurement, and Control, Vol.124, No.3, pp.398-405, 2002.
- 9) N. Suda, PID Control, Asakurashoten, Tokyo, pp.88-93, 2000.
- 10) <http://www.sgservo.co.kr/index.html>
- 11) <https://kr.mathworks.com/help/xpc/index.html>
- 12) J. Watton, Fundamentals of Fluid Power Control, Cambridge University Cambridge, pp.115-129, 2009.
- 13) I. Istanto, "A Study on Control of Electrohydraulic Servo Valve", Dissertation, Graduate School, Pukyong National University, 2019.
- 14) I. Y. Lee and BRKR, Oil Hydraulic Engineering, 2nd Edition, Munundang Publishing Co., Seoul, 2019.